



Spectroscopic studies on the formation of molecular complexes of sulfamethoxazole with novel 2,3,5-trichloro-6-alkoxy-1,4-benzoquinones

K. Ganesh, C. Balraj, A. Satheshkumar, K.P. Elango*

Department of Chemistry, Gandhigram Rural Institute (Deemed University), Gandhigram 624 302, India

HIGHLIGHTS

- ▶ New 2,3,5-trichloro-6-alkoxy-1,4-benzoquinones were employed as acceptors in CT interaction.
- ▶ The mechanism/structure of the products were characterized using various spectral techniques.
- ▶ Electronic effects of the substituents determine electron accepting property of quinones.

ARTICLE INFO

Article history:

Received 7 July 2012

Received in revised form 23 September 2012

Accepted 24 September 2012

Available online 2 October 2012

Keywords:

Charge transfer

Sulfamethoxazole

Substituent effect

Fluorescence

Theoretical studies

Taft correlation

ABSTRACT

UV–Vis, ^1H NMR, FT-IR, LC–MS and fluorescence spectral techniques were employed to investigate the mechanism of interaction of sulfamethoxazole with alkoxy substituted 2,3,5-trichloro-1,4-benzoquinones and to characterize the reaction products. The interactions of these quinones with sulfamethoxazole (SULF) were found to proceed through the formation of donor–acceptor complex, containing radical anion and its conversion to the product. Fluorescence quenching studies indicated that the interaction between the donor and the acceptors are spontaneous. Correlation of association constants of the CT complexes with Taft's polar and steric constants indicated that polar factor plays a significant role in governing the reactivity. The results indicated that the electronic effects of the substituents play significant role in governing the reactivity of the quinones when compared to steric factor.

© 2012 Elsevier B.V. All rights reserved.

1. Introduction

In recent years considerable attention has been given to study the charge transfer (CT) or electron donor acceptor (EDA) complexes formed between organic donor compounds and σ or π acceptors [1–5]. This growing importance is due its interesting optical and electronic properties [6]. CT phenomenon has enormous applications in the field of organic light emitting diodes [7], organic photovoltaics [8], sensors [9], organic field effect transistor [10], nonlinear optics [11], magnetic materials [11], organic solar cells [12], xerogel nanoparticles [13] and in the quantitative estimation of drugs [14]. Drug–receptor mechanism can also be explained by CT phenomenon in addition to weak interactions such as hydrogen bonding and hydrophobic interactions together with van der Waal's forces like dipole–dipole, dipole induced dipole and dispersion interactions. Understanding the drug–receptor mechanism is a complex issue, but collection of data of the interactions like CT, hydrogen bonding even in organic solvents can shed some light on drug–receptor mechanism [15,16]. As a primary step

to determine whether CT phenomenon at any level involved, the ability of the donor drugs and related compounds to form charge transfer complexes with acceptors should be studied.

Quinones are important class of organic molecules which notably plays an essential role in oxido-reduction reactions such as respiration and photosynthesis [17]. Quinones are capable of accepting one or two electrons to form the corresponding radical anion (Q^-) and hydroquinone dianion (Q^{2-}). The biological activity of the quinones is reportedly due to the redox chemistry of the quinone system [18]. It is well known that a modification in the direct substitution pattern on the quinone ring impact its capability to accept electrons and thus its capacity to mediate biological reactions [19–21]. The key electron acceptors in the photosynthetic processes are menaquinones, plastoquinones and ubiquinones are exist in the form of substituted 1,4-benzoquinone module [22,23]. Also, these naturally occurring quinones possess variable number of alkoxy substituents in their units. Although good amount of work, on the study of charge transfer (CT) complexes of number of quinones with variety of donors, has been carried out [24–27], reports related to quinones with systematic variation of substituents is rare in literature.

* Corresponding author. Tel.: +91 451 245 2371; fax: +91 451 245 4466.

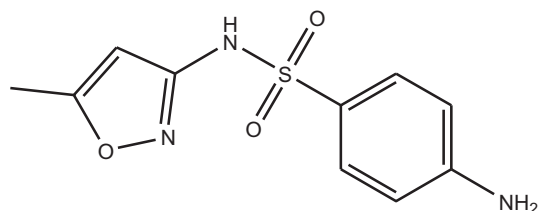
E-mail address: drkpelango@rediffmail.com (K.P. Elango).

Thus, the mechanism of interaction of quinone with drugs, in general, is a research topic of significant interest and hence the present study. The objective, therefore, of the present article is to study the spectral, thermodynamic and kinetic aspects of the interaction of 1,4-benzoquinones with variable alkyl chain of alkoxy groups with sulfamethoxazole (SULF) drug with an aim to investigate the mechanism of the interaction and to characterize the structure of the products formed in these interactions. In general, drugs are poly-functional organic molecules and the present study aims at to investigate the actual site of attack during the formation of charge transfer complexes. Such a study would undeniably shed some light on to the mechanism of the drug action in real pharmacokinetic study. Sulfamethoxazole is chemically known as 4-amino-*N*-(5-methylisoxazol-3-yl)-benzene sulfonamide which is used as an antibacterial agent and to treat urinary tract infections [27,28]. It can also be used in the treatment of sinusitis, toxoplasmosis and pneumocystis pneumonia which affects primarily patients with HIV. Though these chosen 1,4-benzoquinones are known to organic chemists as intermediates, it is the first systematic attempt to utilize them as acceptors with the drug. Such a structural variation of the quinones would certainly help to tune the redox chemistry of them and hence its biological activity. Attempts have also been made to investigate the effect of substituents on the CT interaction using the techniques of correlation analysis by employing Taft's substituent constants.

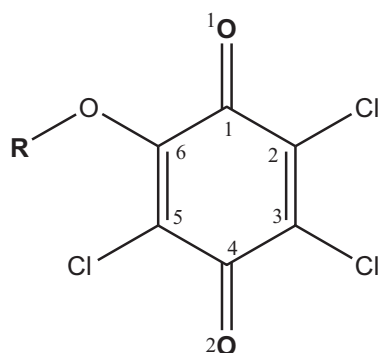
2. Experimental

2.1. Material and methodology

The electron acceptors viz. alkoxy substituted 1,4-benzoquinones were synthesized and purified by the reported method [29]. The electron donor sulfamethoxazole was obtained as gift sample from a locally available pharmaceutical company and was used as received. The purity of the drug was checked by its melting point (observed 169 °C; literature 169 °C), ^1H NMR and FT-IR spectra. Commercially available spectroscopic grade solvents (Merck, India) were used without further purification. The structures of the drug and the acceptors are shown below.



Chemical structure of Sulfamethoxazole



Where R= Methyl (MQ); Ethyl (EQ); Isopropyl (IPQ) and n-butyl (BQ)

Solutions for the spectroscopic measurements were prepared by dissolving accurately weighed amounts of donor (D) and acceptor (A) in the appropriate volume of solvent immediately before running the spectra. The electronic absorption spectra were recorded on a JASCO (V 630, Japan) UV-Vis double beam spectrophotometer using 1 cm matched quartz cells by using corresponding pure solvent as reference. The temperature of the cell holder was controlled with a water flow (0.2 °C). The steady state fluorescence spectra were obtained on a JASCO (FP 6200, Japan) spectrofluorimeter. The emission slit width (5 nm) and the scan rate (250 nm) was kept constant for all of the experiments. FT-IR spectra were recorded in a JASCO (FT-IR 460 Plus, Japan) spectrometer by using KBr pellet. ^1H NMR spectra were recorded at Madurai Kamaraj University, Madurai in a Bruker NMR spectrometer (300 MHz, Switzerland) using TMS as internal standard and DMSO- d_6 as solvent at room temperature. The LCMS spectra were obtained from University of Hyderabad in a Shimadzu (LCMS 2010) spectrophotometer with ionization potential at 70 eV (LCMS 2010, Japan). Elemental analyses for CHN was performed at Sophisticated Analytical Instrument Facility, Cochin University of Science and Technology, Kochi (Elementar Vario EL III, Germany).

2.2. Synthesis and characterization of substituted quinones

1,4-Benzoquinones possessing varying number of chloro and alkoxy substituents were synthesized and purified as reported elsewhere [29]. An excess amount of corresponding sodium alkoxide was added into a stirred solution of chloranil in the respective solvent at RT under N_2 atm. The reaction mixture was stirred for 12 h at 70 °C or 90 °C and cooled to room temperature. Then the reaction mixture was added into 200 ml of water and stirred for 1 h at RT. The crude material formed was filtered through a filter paper and residue was purified using column chromatography (Silica gel 60–120 by using 5–10% ethyl acetate pet ether mixture). The percentage yields of various quinones obtained by this method are shown in Scheme 1.

2.2.1. 2,3,5-Trichloro-6-methoxycyclohexa-2,5-diene-1,4-dione (MQ)

^1H NMR (DMSO- d_6 , 300 MHz; Fig. 1Sa), δ (ppm) 4.19 (s, 3H), FT-IR (KBr, cm^{-1}): 1680 (C=O), 1668 (C=O), 1567 (C=C), UV-Vis in ethanol (λ_{max}): 419 nm ($n \rightarrow \pi^*$), $\log \epsilon$ 2.50, Anal. Calcd. for $\text{C}_7\text{H}_3\text{Cl}_3\text{O}_3$: C, 34.82; H, 1.25; found: C, 36.17; H, 1.74; m.p. 172 °C.

2.2.2. 2,3,5-Trichloro-6-ethoxycyclohexa-2,5-diene-1,4-dione (EQ)

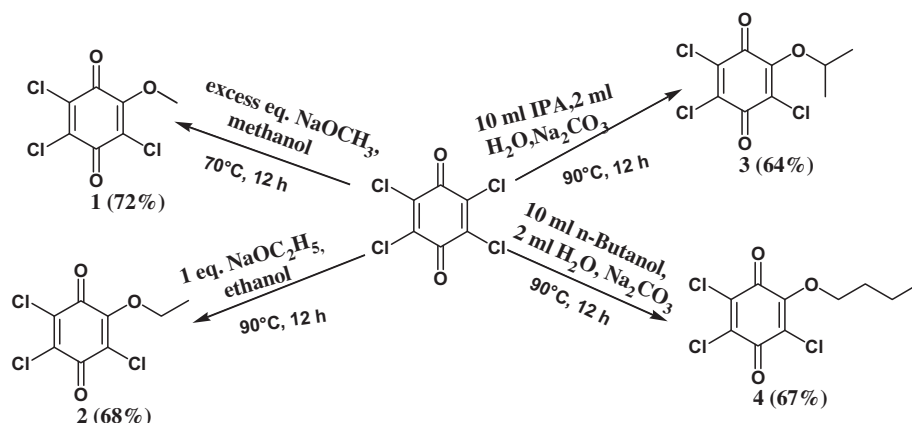
^1H NMR (DMSO- d_6 , 300 MHz, Fig. 1Sb), δ (ppm) 1.39 (t, $J = 7.20$ Hz, 3H), 4.45–4.53 (m, 2H); FT-IR (KBr, cm^{-1}): 1676, 1608 (C=O); UV-Vis in ethanol (λ_{max}): 419 nm, $\log \epsilon$ 2.62, Anal. Calcd. for $\text{C}_8\text{H}_5\text{Cl}_3\text{O}_3$: C, 37.61; H, 1.97; found: C, 36.87; H, 1.84; m.p. 112 °C.

2.2.3. 2,3,5-Trichloro-6-isopropoxycyclohexa-2,5-diene-1,4-dione (IPQ)

^1H NMR (DMSO- d_6 , 300 MHz, Fig. 1Sc), δ (ppm) 1.34 (d, $J = 6.00$ Hz, 6H), 4.98–5.10 (m, 1H); FT-IR (KBr, cm^{-1}): 1670, 1648 (C=O), UV-Vis in ethanol (λ_{max}): 419 nm, $\log \epsilon$ 2.62, Anal. Calcd. for $\text{C}_9\text{H}_7\text{Cl}_3\text{O}_3$: C, 40.11; H, 2.62; found: C, 40.81; H, 2.56; m.p. 74 °C.

2.2.4. 2,3,5-Trichloro-6-butoxycyclohexa-2,5-diene-1,4-dione (BQ)

^1H NMR (DMSO- d_6 , 300 MHz, Fig. 1Sd), δ (ppm) 0.9 (t, $J = 6.00$ Hz, 3H), 1.35–1.48 (m, 2H), 1.63–1.74 (m, 2H), 4.45 (t, $J = 6.30$ Hz, 2H); FT-IR (KBr, cm^{-1}): 1672, 1649 (C=O), UV-Vis in ethanol (λ_{max}): 419 nm, $\log \epsilon$ 2.62, Anal. Calcd. for $\text{C}_{10}\text{H}_9\text{Cl}_3\text{O}_3$: C, 42.36; H, 3.20; found: C, 42.14; H, 3.18; m.p. 88 °C.



Scheme 1. Preparation method for alkoxy substituted quinones.

2.3. Characterization of reaction products

In all the cases, the reaction products were obtained by allowing the reactants to react for 24 h under stoichiometric conditions (4 mmol of SULF and 4 mmol of corresponding acceptors in ethanol) and subjected to MPLC separation. The products were characterized using analytical (CHN) and spectral techniques viz. ^1H NMR [(Figs. 3Sa, 3Sb, 3Sc, and 3Sd; supplemental information), FT-IR [(Figs. 4Sa, 4Sb, 4Sc and 4Sd; supplemental information)] and LC-MS [(Figs. 5Sa, 5Sb, and 5Sc; supplemental information)].

2.3.1. SULF-MQ [2,5-dichloro-6-methoxy-3-(4-amino-N-(5-methylisoxazol-3-yl)-benzene sulfonamide) cyclohexa-2,5-diene-1,4-dione]

^1H NMR (DMSO- d_6 , 300 MHz), δ (ppm) 2.29 (s, 3H), 4.17 (s, 3H), 6.14 (s, 1H), 7.14 (d, $J = 8.70$ Hz, 2H), 7.72 (d, $J = 8.70$ Hz, 2H), 9.62 (s, 1H), 11.33 (s, 3H). FT-IR (KBr, cm^{-1}): 3249 (N–H), 1671 (C=O), 1265, 1037 (–OCH₃); LCMS: Calcd. For $\text{C}_{17}\text{H}_{13}\text{Cl}_2\text{N}_3\text{O}_6\text{S}$: 458.2; found: 458.4; Anal. Calcd. for $\text{C}_{17}\text{H}_{13}\text{Cl}_2\text{N}_3\text{O}_6\text{S}$: C, 44.55; H, 2.86; N, 9.17; found: C, 44.75; H, 2.70; N, 9.06.

2.3.2. SULF-EQ [2,5-dichloro-6-ethoxy-3-(4-amino-N-(5-methylisoxazol-3-yl)-benzene sulfonamide) cyclohexa-2,5-diene-1,4-dione]

^1H NMR (DMSO- d_6 , 300 MHz), δ (ppm) 1.31 (t, 3H), 2.29 (s, 3H), 4.47 (m, 2H), 6.14 (s, 1H), 7.15 (d, $J = 8.70$ Hz, 2H), 7.72 (d, $J = 8.70$ Hz, 2H), 9.61 (s, 1H), 11.33 (s, 3H). FT-IR (KBr, cm^{-1}): 3224 (N–H), 1671 (C=O), 1278, 1035 (–OCH₃); LCMS: Calcd. For $\text{C}_{18}\text{H}_{15}\text{Cl}_2\text{N}_3\text{O}_6\text{S}$: 472.3; found: 472.3; Anal. Calcd. for $\text{C}_{18}\text{H}_{15}\text{Cl}_2\text{N}_3\text{O}_6\text{S}$: C, 45.77; H, 3.20; N, 8.90; found: C, 45.75; H, 3.17; N, 8.87.

2.3.3. SULF-IPQ [2,5-dichloro-6-isopropoxy-3-(4-amino-N-(5-methylisoxazol-3-yl)-benzene sulfonamide) cyclohexa-2,5-diene-1,4-dione]

^1H NMR (DMSO- d_6 , 300 MHz), δ (ppm) 1.32 (d, $J = 6.00$ Hz, 6H), 2.29 (s, 3H), 4.99 (m, 1H), 6.14 (s, 1H), 7.16 (d, $J = 8.70$ Hz, 2H), 7.72 (d, $J = 8.70$ Hz, 2H), 9.61 (s, 1H), 11.33 (s, 3H). FT-IR (KBr, cm^{-1}): 3222 (N–H), 1670 (C=O), 1274, 1025 (–OCH₃); LCMS: Calcd. For $\text{C}_{19}\text{H}_{17}\text{Cl}_2\text{N}_3\text{O}_6\text{S}$: 486.3; found: 486.3; Anal. Calcd. for $\text{C}_{19}\text{H}_{17}\text{Cl}_2\text{N}_3\text{O}_6\text{S}$: C, 46.92; H, 3.52; N, 8.64; found: C, 46.87; H, 3.49; N, 8.63.

2.3.4. SULF-BQ [2,5-dichloro-6-butoxy-3-(4-amino-N-(5-methylisoxazol-3-yl)-benzene sulfonamide) cyclohexa-2,5-diene-1,4-dione]

^1H NMR (DMSO- d_6 , 300 MHz), δ (ppm) 0.90 (t, 3H), 1.40 (m, 2H), 1.64 (m, 2H), 2.29 (s, 3H), 4.45 (t, 2H), 6.15 (s, 1H), 7.15 (d, $J = 8.70$ Hz, 2H), 7.72 (d, $J = 8.70$ Hz, 2H), 9.61 (s, 1H), 11.33 (s, 3H). FT-IR (KBr, cm^{-1}): 3220 (N–H), 1670 (C=O), 1263, 1033 (–OCH₃); LCMS: Calcd. For $\text{C}_{20}\text{H}_{19}\text{Cl}_2\text{N}_3\text{O}_6\text{S}$: 499.0; found: 499.0; Anal. Calcd. for $\text{C}_{20}\text{H}_{19}\text{Cl}_2\text{N}_3\text{O}_6\text{S}$: C, 48.01; H, 3.83; N, 8.40; found: C, 47.97; H, 3.81; N, 8.36.

2.4. Kinetic procedure

The kinetics of the interaction of SULF with the acceptors (MQ, EQ, IPQ and BQ) different quinones was followed at three different temperatures in ethanol solvent under pseudo-first-order conditions, keeping $[D] \gg [A]$. The increase in absorbance of the new peak at 340 nm for with elapse of time was recorded. The pseudo-first-order rate constants (k_1) were calculated from the gradients of $\log -(A_\infty - A_t)$ against time plots, where A_∞ and A_t represent the absorbance at infinity and time t , respectively. The second order rate constants were calculated by dividing k_1 by $[D]$ [5].

2.5. Theoretical studies

The geometrical optimization of the donor SULF and the quinones MQ, EQ, IPQ and BQ was performed by using Density Functional Theory method with the B3LYP hybrid functional, of 6-31G basis sets with the Gaussian 03 Revision D.01 program package, 2004.

3. Results and discussion

3.1. Stoichiometry of the interaction

The stoichiometry of the CT complex formed, in all the cases, was determined by applying Job's continuous variation method [30]. In all the cases (SULF-MQ, SULF-EQ, SULF-IPQ, SULF-BQ) the symmetrical curve with a maximum at 0.5 mol fraction indicated the formation of a 1:1 (D:A) CT complex [(Fig. 6Sa) Supplemental information]. The photometric titration measurements were also performed for the determination of the stoichiometry in these interactions. The results of the photometric titration studies [(Fig. 6Sb) Supplemental information] confirmed the observed stoichiometry of the interaction [31]. The stoichiometry of the SULF-MQ, SULF-EQ, SULF-IPQ, SULF-BQ systems is further confirmed by Jobs continuous variation method using emission studies also [32] [(Fig. 6Sc) Supplemental information].

3.2. Characterization of reaction products

The FT-IR spectra of the pure SULF, MQ, EQ, IPQ, BQ and their products (SULF-MQ, SULF-EQ, SULF-IPQ and SULF-BQ) were recorded and the peak assignments for important peaks are given in [(Tables 1Sa–1Sd, Supplemental Information)]. The results indicated that the shifts in positions of some of the peaks could be attributed to the symmetry and electronic structure modifications

in both donor and acceptor units in the formed product relative to the free molecules.

For a representative case, in SULF-MQ system, some of the significant shifts are: the peak due to asymmetric and symmetric —NH_2 vibrations of the free SULF occurred at 3469 cm^{-1} and 3376 cm^{-1} respectively and in SULF-MQ product it appeared at 3249 cm^{-1} indicating the participation of N—H moiety in product formation. The $\nu(\text{C=O})$, $\nu(\text{O—CH}_3)$ and $\nu(\text{C—Cl})$ stretching vibrations in the free MQ species appeared at 1684 , 1270 and 909 cm^{-1} respectively. In the product these stretching vibrations occurred at 1671 , 1265 and 896 cm^{-1} , respectively. Such a bathochromic shift could be indicative of a higher charge density on the carbonyl group of the MQ molecule [26].

As a representative case, the ^1H NMR spectra of the donor SULF and its reaction product with MQ were recorded in $\text{DMSO-}d_6$ and are given in [(Figs. 2S and 3Sa Supplemental Information)] respectively. Using the proton NMR technique, we can identify the nature of interaction between the donor and acceptor in the resulted product. Pure SULF molecule exhibited the characteristic peak due to aromatic —NH_2 group at 6.087 ppm and in the product it appeared at 9.620 ppm as —NH group. This observation indicated that the product between SULF and MQ is formed with the elimination of HCl molecule. It is also interesting to note that the —NH protons, in the corresponding product, appeared at 9.620 , 9.614 , 9.610 and 9.613 ppm for MQ, EQ, IPQ and BQ systems, respectively. This indicated that the order of the strength of the acceptors is $\text{MQ} > \text{EQ} > \text{BQ} > \text{IPQ}$. This is because of the fact that greater is the electron accepting power of the acceptor, greater is the acidity of the —NH proton directly attached to the quinone ring. The aromatic protons of pure SULF molecule lie in the range of $6.562\text{--}7.475\text{ ppm}$ and in the product they lie in the range of $7.144\text{--}7.754\text{ ppm}$. The —NH proton of the pure SULF occurs at 10.927 ppm and in the product it occurs at 11.339 ppm . The down field shifts of most of the signals are corresponding due to the interaction occurred between the donor and the acceptor [5,33].

The LCMS spectrum, of SULF-MQ product was recorded and it exhibited the molecular ion peak at m/z 458 (Fig. 5a) which confirms the chemical reaction between the donor and acceptor leading to the product. In the SULF-EQ and SULF-IPQ cases, the molecular ion peaks at m/z 472 and 486 respectively confirmed the product formation between SULF and the corresponding acceptors. [(Fig. 5sa, 5sb and 5sc. Supplemental information)].

3.3. Interaction of sulfamethoxazole with the acceptors

The electronic spectra of MQ in the presence of large excess of donor i.e. $[D]/[A] > 100$ were recorded as a function of time in ethanol (Fig. 1). Immediately after mixing ethanolic solutions of colorless SULF and pale yellow colored MQ, yields a pink colored solution whose electronic spectrum showed absorption band in the $460\text{--}600\text{ nm}$ range. This is the characteristic absorption bands of quinone radical ion [34–36]. It is observed that with elapse of time the intensity of these bands decreased (Fig. 1 inset) with a

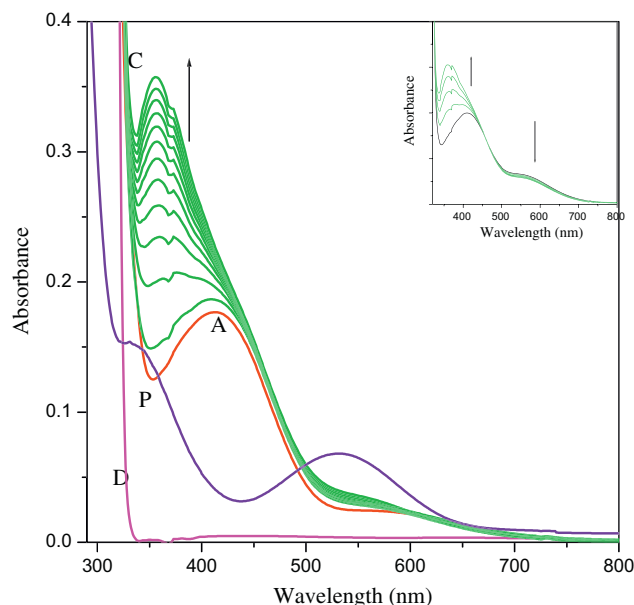


Fig. 1. Electronic absorption spectra of SULF with MQ in ethanol at 298 K (D: Donor; A: Acceptor; C: complex; P: product) Inset: clear isosbestic point at 456 nm.

concurrent increase in intensity of a band at 418 nm . A clear isosbestic point is observed at 456 nm . The position of the absorption maximum of the peak at 418 nm has also been blue shifted with elapse of time. These observations indicated that the initial reactants were converted into final product via radical ion formation. For comparison the electronic spectrum of the product is also shown in Fig. 1. In other cases (SULF-EQ, IPQ and BQ systems), also on mixing the ethanolic solutions of the reactants, similar pattern of electronic spectra were observed. The electronic spectra of all the systems are shown in [(Figs. 7Sa, 7Sb and 7Sc) Supplemental Information].

The kinetics of the interaction of SULF with the acceptors has been followed by monitoring the increase in absorbance of the new peak in ethanol as a function of time under pseudo-first-order conditions i.e. $[D] > [A]$. The pseudo-first-order rate constant (k_1) values for the formation of the product as a function of $[D]$ and $[A]$ are collected in Table 1. It is evident from the results that in all the cases, the rate constant is independent of initial concentration of $[A]$ indicating first order dependence on $[A]$. In all the cases the plot of $\log k_1$ versus $\log [D]$ is linear with a slope of unity ($r > 0.995$; slope range $0.845\text{--}0.912$) [(Fig. 8S) Supplemental Information] indicating unit order dependence on $[D]$. This was further supported by the constancy in k_2 values [34].

The pseudo first-order rate constants, for all the systems, were measured at three different temperatures and the thermodynamic parameters computed are collected in Table 2. A large negative value of entropy of activation indicated the involvement of polar

Table 1
Effect of concentration of donor and acceptors on the rate of the interaction at 298 K.

$[D]$ (10^{-2} M)	$[A]$ (10^{-4} M)	k_1 (10^{-4}), (s^{-1})				k_2 ($\text{s}^{-1}\text{ mol}^{-1}\text{ dm}^3$)			
		SULF-MQ	SULF-EQ	SULF-IPQ	SULF-BQ	SULF-MQ	SULF-EQ	SULF-IPQ	SULF-BQ
0.5	5.5	1.65	1.47	1.18	1.42	3.4	2.9	2.3	2.8
0.7	5.5	2.45	2.08	1.65	1.95	3.5	3.0	2.3	2.8
0.9	5.5	3.12	2.76	2.12	2.61	3.4	3.0	2.3	2.9
1.1	5.5	3.76	3.25	2.54	3.17	3.4	3.0	2.3	2.8
1.1	4.4	3.06	2.74	1.89	2.29				
1.1	3.3	3.06	2.70	1.89	2.29				
1.1	2.2	3.06	2.71	1.89	2.29				

Table 2

Kinetic and thermodynamic parameters for the interaction of SULF with the acceptors in ethanol.

System	λ (nm)	k_1 (10^{-4}) (s^{-1})			ΔH^\ddagger	$-\Delta S^\ddagger$	ΔG^\ddagger
		298	305	313 K			
SULF-MQ	355	3.76	4.70	5.60	17	250	93
SULF-EQ	355	3.26	4.47	5.72	26	223	93
SULF-IPQ	355	2.54	3.90	4.72	29	216	93
SULF-BQ	355	3.17	4.56	5.12	23	235	93

ΔH^\ddagger , kJ mol $^{-1}$; ΔS^\ddagger , J K $^{-1}$ mol $^{-1}$; ΔG^\ddagger , kJ mol $^{-1}$.

transition state. This may be due to the fact that there is some charge separation in the transformation of the reactants to product. Also the negative entropy of activation indicated a greater degree of ordering in the transition state than in the initial state, due to an increase in solvation during the activation process.

Based on the foregoing results and discussions the following plausible mechanism for the interaction SULF with acceptors has been proposed (Scheme 2).

3.4. Characteristics of the CT complexes

In all the cases, an attempt was made to characterize the CT complexes formed in these reactions. For that the absorbance of

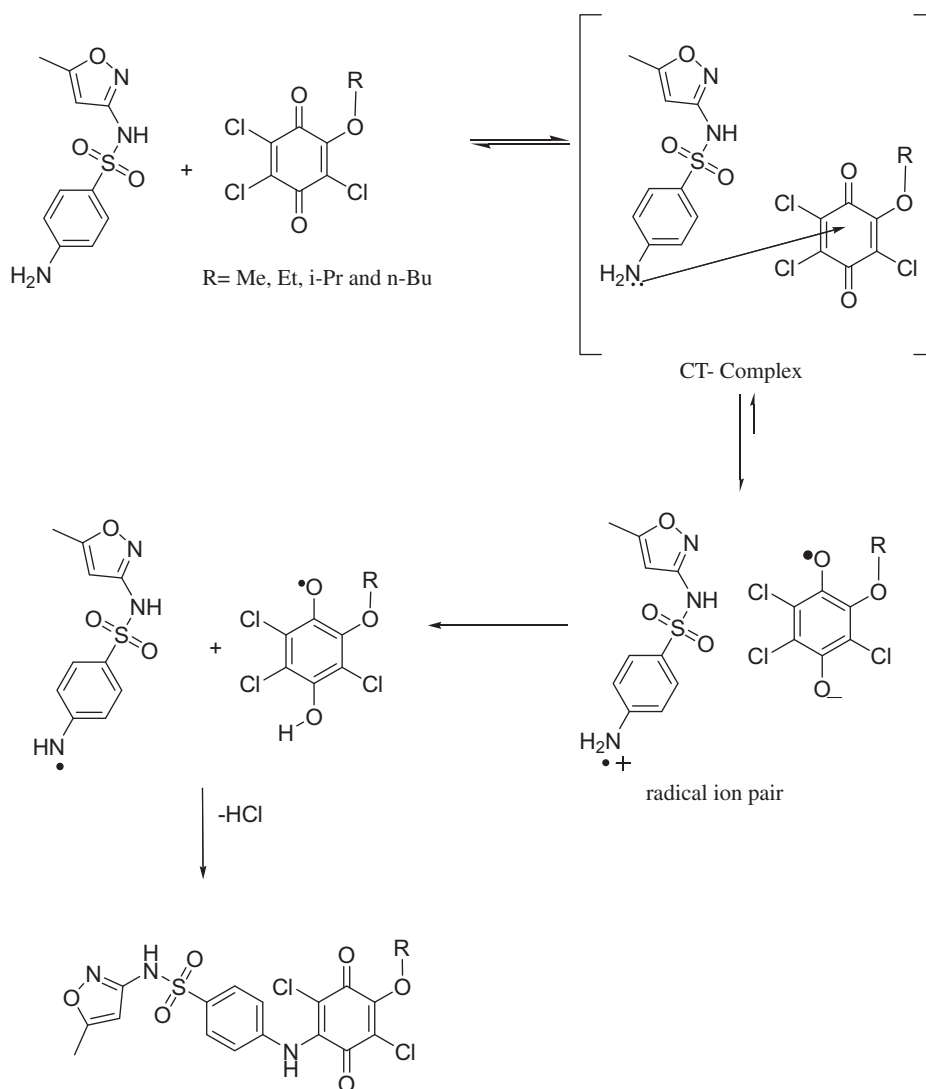
the new bands were measured using constant acceptor concentration in ethanol solvent and varying concentrations of the donor but always $[D] \gg [A]$. Representative spectra for SULF-MQ system is shown in [(Fig. 9S supplemental information)]. The nature of the spectra indicated that the interactions between the donor and the acceptor are of CT type. The formation constants (K) and molar extinction coefficients (ϵ) of the CT complexes were determined spectrophotometrically using the Scott equation [37].

$$[D][A]/d \approx [D]/\epsilon + (1/K\epsilon) \quad (1)$$

where $[D]$ and $[A]$ are the initial molar concentration of the donor and acceptor, respectively and d the absorbance. The values of K and ϵ are determined from the gradient and intercept of the linear plot of $[D][A]/d$ against $[D]$. Representative Scott plots are shown in [(Fig. 10S) Supplemental Information] and the values of K and ϵ thus determined are given in Table 3. The observed high values of K suggested that the formed CT complexes are of a strong type [34] and the linearity of the Scott plots further supports this result.

3.5. Fluorescence studies

The nature and magnitude of the interaction of drugs with receptors play an important role in the pharmacokinetics of the drugs. CT interaction is one of the non covalent binding forces in

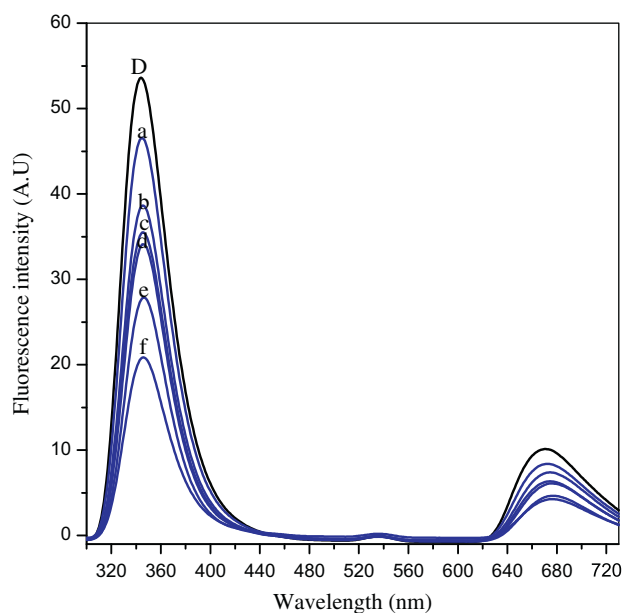
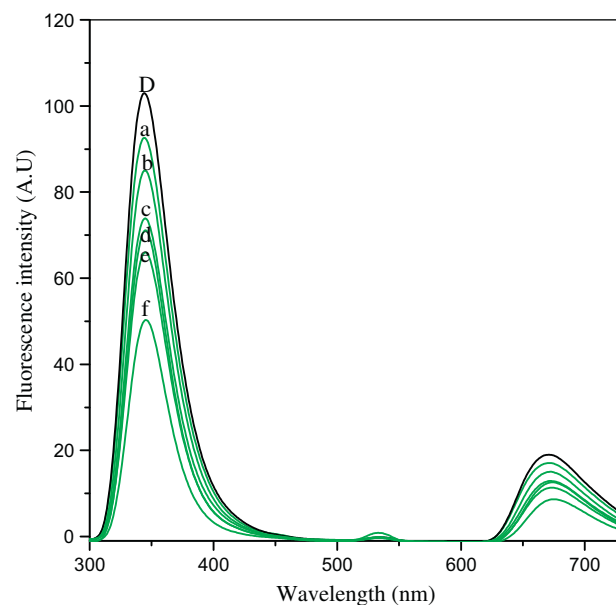
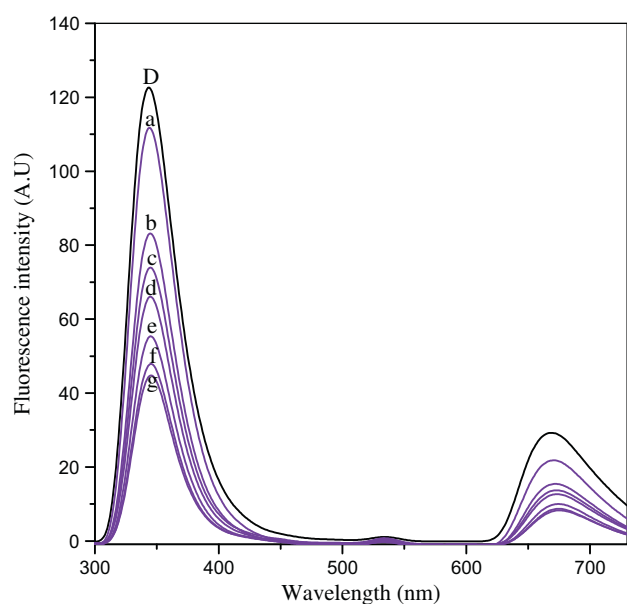
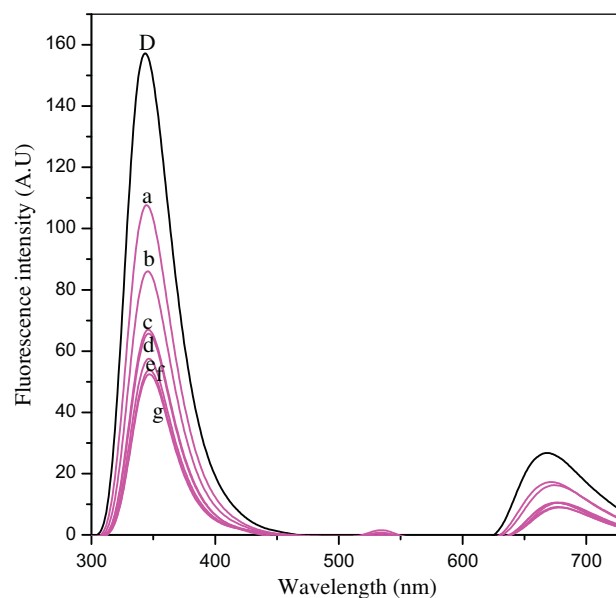


Scheme 2. Mechanism of interaction of SULF with the acceptors.

Table 3

Spectral properties of the CT complexes formed between sulfamethoxazole and the acceptors in ethanol at 298 K.

Property	SULF-MQ	SULF-EQ	SULF-IPQ	SULF-BQ
Formation constant K ($\text{dm}^3 \text{mol}^{-1}$) Abs method	2980	2600	2040	2140
Extinction coefficient $\log \epsilon$ ($\text{dm}^3 \text{mol}^{-1} \text{cm}^{-1}$) Abs method	3.806	3.725	3.641	3.698
Association constant K_f (mol L^{-1}) emission method	3615	2083	1268	1982
Stern–Volmer constant K_{SV} emission method	3891	2001	1643	1991

**Fig. 2.** Variation of fluorescence spectra of SULF-MQ system in ethanol at fixed concentration $[D] = [2.8125 \times 10^{-3}]$ (curve D) and variable concentration of $[A] \times 10^{-4} = \{1.3875$ (curve a), 2.775 (curve b), 4.1625 (curve c), 5.55 (curve d), 6.9375 (curve e), 8.325 (curve f) mol L^{-1} at 298 K.**Fig. 4.** Variation of fluorescence spectra of SULF-IPQ system in ethanol at fixed concentration $[D] = [2.8125 \times 10^{-3}]$ (curve D) and variable concentration of $[A] \times 10^{-4} = \{1.3875$ (curve a), 2.775 (curve b), 4.1625 (curve c), 5.55 (curve d), 6.9375 (curve e), 8.325 (curve f) mol L^{-1} at 298 K.**Fig. 3.** Variation of fluorescence spectra of SULF-EQ system in ethanol at fixed concentration $[D] = [2.8125 \times 10^{-3}]$ (curve D) and variable concentration of $[A] \times 10^{-4} = \{1.3875$ (curve a), 2.775 (curve b), 4.1625 (curve c), 5.55 (curve d), 6.9375 (curve e), 8.325 (curve f), 9.7125 (curve g) mol L^{-1} at 298 K.**Fig. 5.** Variation of fluorescence spectra of SULF-BQ system in ethanol at fixed concentration $[D] = [2.8125 \times 10^{-3}]$ (curve D) and variable concentration of $[A] \times 10^{-4} = \{1.3875$ (curve a), 2.775 (curve b), 4.1625 (curve c), 5.55 (curve d), 6.9375 (curve e), 8.325 (curve f), 9.7125 (curve g) mol L^{-1} at 298 K.

the drug–receptor mechanism. In the present study, an attempt was made to study the CT interaction of SULF with MQ, EQ, IPQ, and BQ by means of fluorescence study. Fluorescence spectra were recorded at room temperature in ethanol in the range of 300–700 nm using an excitation at 270 nm for SULF. It was observed that the fluorescence of SULF was quenched by these acceptors as a result of formation of CT complex. The experimental results indicated that the quenching efficiency increased with increasing concentration of the electron acceptor (Figs. 2–5) and with increasing time. The fraction of acceptors bound to the donor was determined by using the following equation.

$$\theta = (F_0 - F)/F_0 \quad (2)$$

where F and F_0 denote the fluorescence intensities of donor in the presence of acceptor and in the absence of acceptor, respectively. From the resulting values of θ , the association constant K_f for SULF-MQ, SULF-EQ, SULF-IPQ and SULF-BQ systems was computed using the method described by Ward [38]. It has been shown that for equivalent and independent binding sites

$$1/(1 - \theta)K_f = [A_T]/\theta - n[D_T] \quad (3)$$

where n is the number of binding sites, $[A_T]$ is the total acceptor concentration and $[D_T]$ is the total donor concentration. For all the cases the plots $1/(1 - \theta)$ versus $[A_T]/\theta$ are linear ($r > 0.97$) indicating that under the experimental conditions all the binding sites are equivalent and independent. The value of K_f obtained, from the plots, for SULF-MQ, SULF-EQ, SULF-IPQ and SULF-BQ systems are found to be 3.6×10^3 , 2.1×10^3 , 1.2×10^3 and 1.9×10^3 mol L⁻¹, respectively. The standard Gibbs energy change ΔG° was calculated from the K_f values using the relation $\Delta G^\circ = -2.303 RT \log_{10} K_f$. The ΔG° values for SULF-MQ, SULF-EQ, SULF-IPQ and SULF-BQ systems were found to be -19.6 , -18.3 , -17.1 and -18.1 kJ mol⁻¹ respectively, indicating that the interaction between the drug and the acceptors is spontaneous in nature.

Fluorescence quenching can occur by different mechanisms viz. static or dynamic or both. The Stern–Volmer equation (Eq. (4)) is useful in understanding the mechanism of fluorescence quenching.

$$F_0/F = 1 + K_{SV}[Q] \quad (4)$$

where F_0 is the initial fluorescence intensity measured in the absence of quencher and F is that in the presence of quencher concentration $[Q]$. The Stern–Volmer constant K_{SV} is obtained by plotting F_0/F against $[Q]$. In all the cases, linear Stern–Volmer relationship observed (Fig. 6) indicated that either static or dynamic quenching is dominant [39,40].

The relationship between the fluorescence quenching intensity and the concentration of quenchers can be described by the following equation.

$$\log_{10}(F_0 - F)/F = \log K_A + n \log_{10}[Q] \quad (5)$$

where K_A is the binding constant and n is the number of binding sites per donor molecule [41]. In the present study, in all the cases, a plot of $\log_{10}(F_0 - F)/F$ versus $\log_{10}[Q]$ is linear ($r > 0.981$, Fig. 7) and the binding constant values computed are collected in Table 4. The results indicated the magnitude of binding constant is in the order of SULF-MQ > SULF-EQ > SULF-BQ > SULF-IPQ. These observations are in corroboration with the results of absorption spectral and kinetic studies as enumerated earlier in this paper. That is the formation and rate constant computed using absorption spectral data follows the same order (Tables 2 and 3). The value of n , for these systems, is nearly constant in ethanol indicating the presence of equivalent binding sites.

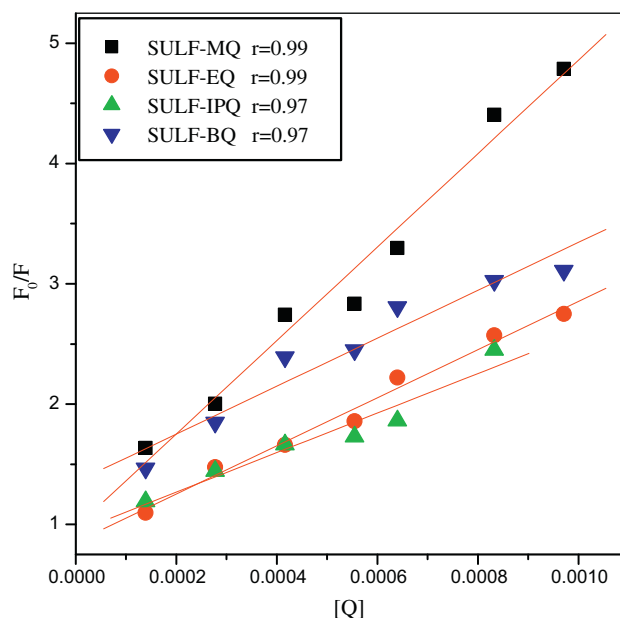


Fig. 6. Stern–Volmer plot for the fluorescence quenching of SULF with MQ, EQ, IPQ and BQ in ethanol at 298 K.

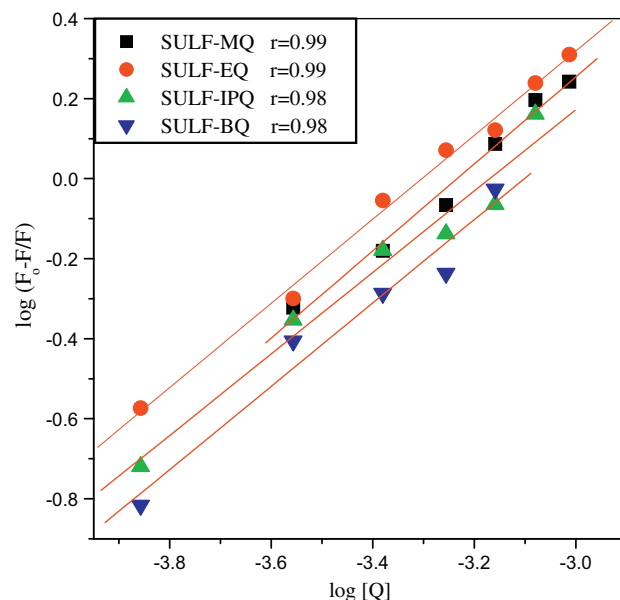


Fig. 7. Plot of $\log (F_0 - F)/F$ versus $\log [Q]$ of SULF with MQ, EQ, IPQ and BQ in ethanol at 298 K.

Table 4
Binding constants (K_A) and number of binding sites (n) for SULF-MQ, SULF-EQ, SULF-IPQ and SULF-BQ systems in ethanol solvent.

Acceptors	K_A (mol ⁻¹ L)	n
SULF-MQ	3.2×10^3	1.1
SULF-EQ	2.9×10^3	1.0
SULF-IPQ	1.5×10^3	1.0
SULF-BQ	1.6×10^3	0.9

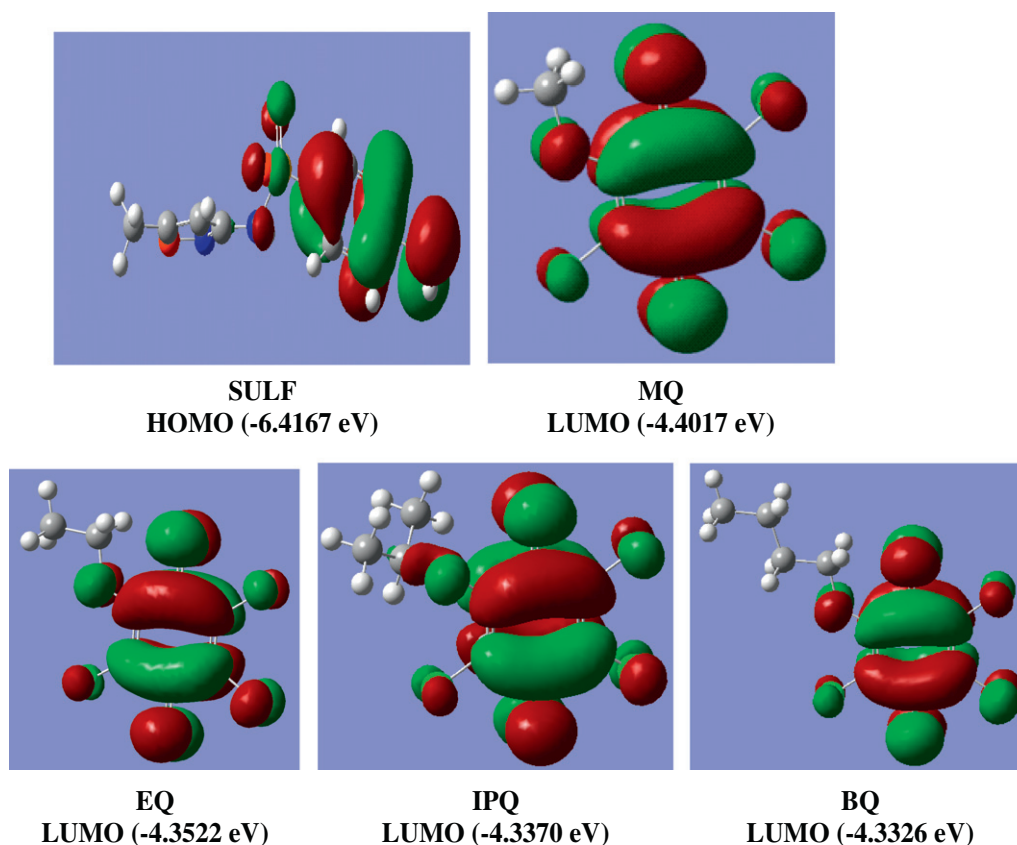


Fig. 8. The optimized structures of the SULF, MQ, EQ, IPQ and BQ along with frontier orbitals.

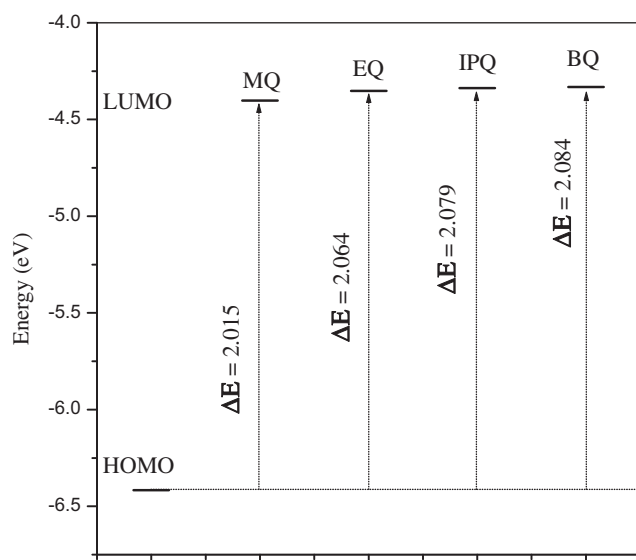


Fig. 9. Energy of HOMO of the donor and LUMO of the acceptors.

3.6. Theoretical calculations

To understand the foregoing experimental observations on the CT complex formed between SULF and the acceptors, we have performed the optimization of structures using Density Functional Theory. Computations have been performed using the Gaussian 03 Revision D.01 program package [42]. The optimized geometry of

the donor along with HOMO and the acceptors along with LUMO are depicted in Fig. 8. In the case of SULF, the HOMO is concentrated on the $-\text{NH}_2$ group and in the case of the acceptors the LUMO resides on the carbonyl group of the quinone ring. The energies of the frontier orbitals of the donor and the acceptors along with the energy corresponds to the CT transition, $\Delta E = (\text{HOMO}_{\text{SULF}} - \text{LUMO}_{\text{acceptor}})$ [43,44], for all the systems, are shown in Fig. 9. It is evident from the figure that the ΔE depends on the nature of the substituent present in the quinone.

3.7. Correlation analysis

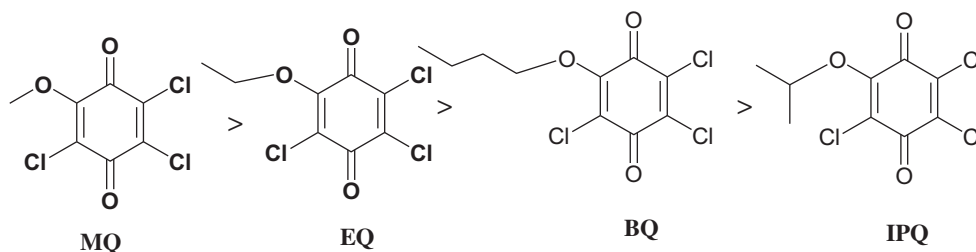
A preliminary attempt has been made to correlate the results (i.e. association constants, K_f) with Taft's polar and steric constants [45]. The results of the correlation analysis are shown below:

$$K_f = 12310\sigma^* + 3529 \quad (r = 0.99; n = 4) \quad (6)$$

$$K_f = -3498E_s + 3050 \quad (r = 0.83; n = 4) \quad (7)$$

A good correlation obtained, between the association constant of the CT complexes and the Taft's polar constant (Eq. (6)), indicated that the electronic effects of the substituents play significant role in governing the reactivity of the quinones when compared to steric factor which showed poor correlation (Eq. (7)). The positive correlation observed between K_f and σ^* (Eq. (6)) indicated that with an increase in electron releasing power of the alkoxy substituent, the quinone becomes increasingly a weaker acceptor.

The above observations indicated that the strength of the acceptor decrease in the order:



4. Conclusions

The charge transfer properties of these 1,4-benzoquinones possessing varying alkoxy substituents were investigated. Various spectral techniques have been employed to characterize the final product of these interactions. In all the cases, the stoichiometry of the CT interaction was found to be 1:1. The trends in the rate constants and formation constants showed that the strength of the complex formation is in the order of SULF-MQ > SULF-EQ > SULF-BQ > SULF-IPQ. The observed equilibrium and kinetic properties of these acceptors were found to be well supported by theoretical calculation studies.

Acknowledgement

The authors thank the University Grants Commission, New Delhi for its financial assistance to carry out this research work.

Appendix A. Supplementary material

Supplementary data associated with this article can be found, in the online version, at <http://dx.doi.org/10.1016/j.molstruc.2012.09.062>.

References

- [1] A. Mostafa, H.S. Bazzi, *Spectrochim. Acta Part A* 79 (2011) 1613.
- [2] S.Y. AlQaradawi, A. Mostafa, H.S. Bazzi, *J. Mol. Struct.* 1011 (2012) 172.
- [3] K. Ganesh, K.P. Elango, *Spectrochim. Acta Part A* 93 (2012) 185.
- [4] M.S. Refat, *J. Mol. Struct.* 985 (2011) 380.
- [5] C. Balraj, K. Ganesh, K.P. Elango, *J. Mol. Struct.* 998 (2011) 110.
- [6] B. Illescas, N. Martin, J.L. Segura, C. Seoane, E. Orti, P.M. Viruela, R. Viruela, *J. Org. Chem.* 60 (1995) 5643.
- [7] Zhong-Fu. An, Run.-Feng. Chen, Jun. Yin, Guo.-Hua. Xie, *Chem. Eur. J.* 17 (2011) 10871.
- [8] Y.J. Cheng, S.H. Yang, C.S. Hsu, *Chem. Rev.* 109 (2009) 5868.
- [9] F. Jakle, *Chem. Rev.* 110 (2010) 3985.
- [10] M.M. Durban, P.D. Kazarinoff, C.K. Luscombe, *Macromolecules* 43 (2010) 6348.
- [11] T.D. Selby, K.R. Stickley, S.C. Blackstock, *Org. Lett.* 2 (2010) 171.
- [12] L. Orian, S. Carlotto, M.D. Valentin, A. Polimeno, *J. Phys. Chem. A* 116 (2012) 3926.
- [13] F. Chaput, F. Lerouge, S.T. Nenez, P.E. Coulon, C. Dujardin, S.D. Quanguin, F. Mpambani, S. Parola, *Langmuir* 27 (2011) 5555.
- [14] A.A. Gouda, *Talanta* 80 (2009) 151.
- [15] A.K. Raza Khan, S. Ahamad Khan, M. Ansari, *Med. Chem. Res.* 20 (2) (2010) 231.
- [16] K. Sharma, S.P. Sharma, S.C. Lahiri, *Spectrochim. Acta Part A* 92 (2012) 212.
- [17] P.H. Bernardo, C.L.L. Chai, M.L. Guen, G.D. Smith, P. Waring, *Bioorg. Med. Chem. Lett.* 17 (2007) 82.
- [18] Wei Ma, Hao Zhou, Yi-Lun Ying, Da-wei Li, Guo.-Rong Chen, Yi-Tao Long, Hong.-Yuan Chen, *Tetrahedron* 67 (2011) 5990.
- [19] N.M. Ruvalcaba, G. Cuevas, I. Gonzalez, M.A. Martinez, *J. Org. Chem.* 67 (2002) 3673.
- [20] Y. Izumi, H. Sawada, N. Sakka, N. Yamamoto, T. Kume, H. Katsuki, S. Shimohama, A. Akaike, *J. Neurosci. Res.* 79 (2005) 849.
- [21] R. Meganathan Vitam, *Harm.* 61 (2001) 173.
- [22] W.W. Li, J. Heinze, W. Haehnel, *J. Am. Chem. Soc.* 127 (2005) 6140.
- [23] A.M. Weyers, R. Chatterjee, S. Milikisyan, K.V. Lakshmi, *J. Phys. Chem. B* 113 (2009) 15409.
- [24] S. Yusif, *Spectrochim. Acta Part A* 78 (2011) 1227.
- [25] E.M. Nour, M.S. Refat, *J. Mol. Struct.* 994 (2011) 289.
- [26] K. Ganesh, C. Balraj, K.P. Elango, *Spectrochim. Acta Part A* 79 (2011) 1621.
- [27] M.S. Refat, S.A. El-Korashy, I.M. El-Deen, S.M. El-Sayed, *J. Mol. Struct.* 980 (2010) 124.
- [28] P.G. Wormser, T.G. Keusch, C.R. Heels, *Drugs* 24 (6) (1982) 459.
- [29] Richard Huot, Paul Brassard, *Can. J. Chem.* 52 (1974) 838.
- [30] P. Job, *Ann. Chim. Phys.* 9 (1928) 113.
- [31] M. Gaber, S.S. Al-Shihry, *Spectrochim. Acta Part A* 62 (2005) 526.
- [32] C.A.T. Laia, S.M.B. Costa, D. Philips, A.W. Parker, *Photochem. Photobiol. Sci.* 2 (2003) 555.
- [33] D.K. Sau, R.J. Butcher, S. Chaudhuri, N. Saha, *Polyhedron* 23 (2004) 5.
- [34] K. Ganesh, C. Balraj, A. Satheshkumar, K.P. Elango, *Spectrochim. Acta Part A* 92 (2012) 46.
- [35] M. Hasani, A. Rezaei, *Spectrochim. Acta Part A* 65 (2006) 1093.
- [36] A.A. Hassan, A.F.E. Mourad, K.M. El-Shaieb, A.H. Abou-Zioud, *Molecules* 10 (2005) 822.
- [37] R.L. Scott, *Recl. Trav. Chim. Pays-Bas Belg.* 75 (1956) 787.
- [38] L.D. Ward, *Method. Enzymol.* 17 (1985) 400.
- [39] J.S. Park, J.N. Wilson, K.I. Hardcastle, U.H.F. Burnz, M. Srinivasarao, *J. Am. Chem. Soc.* 128 (2006) 7714.
- [40] Q. Zhou, T.M. Swager, *J. Am. Chem. Soc.* 117 (1995) 12593.
- [41] H. Xu, Q. Liu, Y. Zuo, Y. Bi, S. Gao, *J. Sol. Chem.* 38 (2009) 15.
- [42] M.J. Frisch, G.W. Trucks, H.B. Schlegel, G.E. Scuseria, M.A. Robb, J.R. Cheeseman, J.A.J. Montgomery, T. Vreven, K.N. Kudin, J.C. Burant, J.M. Millam, S.S. Iyengar, J. Tomasi, V. Barone, B. Mennucci, M. Cossi, G. Scalmani, N. Rega, G.A. Petersson, H. Nakatsuji, M. Hada, M. Ehara, K. Toyota, R. Fukuda, J. Hasegawa, M. Ishida, T. Nakajima, Y. Honda, O. Kitao, H. Nakai, M. Klene, X. Li, J. E. Knox, H.P. Hratchian, J.B. Cross, C. Adamo, J. Jaramillo, R. Gomperts, R.E. Stratmann, O. Yazyev, A.J. Austin, R. Cammi, C. Pomelli, J.W. Ochterski, P.Y. Ayala, K. Morokuma, G.A. Voth, P. Salvador, J.J. Dannenberg, V.G. Zakrzewski, S. Dapprich, A.D. Daniels, M.C. Strain, O. Farkas, D.K. Malick, A.D. Rabuck, K. Raghavachari, J.B. Foresman, J.V. Ortiz, Q. Cui, A.G. Baboul, S. Clifford, J. Cioslowski, B.B. Stefanov, G. Liu, A. Liashenko, P. Piskorz, I. Komaromi, R.L. Martin, D.J. Fox, T. Keith, M.A. I-Laham, C.Y. Peng, A. Nanayakkara, M. Challacombe, P.M.W. Gill, B. Johnson, W. Chen, M.W. Wong, C. Gonzalez, J.A. Pople, *Gaussian 03W Revision D.01*, Gaussian, Inc., Wallingford, CT, 2004.
- [43] N. Cho, J. Kim, K. Song, J.K. Lee, J. Ko, *Tetrahedron* 68 (2012) 4029.
- [44] B. Tejerina, C.M. Gothard, B.A. Grzybowski, *Chem. Eur. J.* 18 (2012) 5606.
- [45] J. Shorter, *Correlation analysis of organic reactivity*, Research Studies Press, New York, 1982.